Original Article

Sulforaphane attenuates phosgene-induced acute lung injury via the Nrf2-HO-1/NQO1 pathway

Qianying Lu[1,2#], Siyu Huang[1,2#], Yanmei Zhao[1,2], Sifan Yu[1,2], Mingyu Shi[1,2], Junfeng Li[1,2], Yangfan Liang[1,2], Haojun Fan[1,2], Shike Hou[1,2]

[1]School of Disaster and Emergency Medicine, Tianjin University, Tianjin, China; [2]Tianjin Key Laboratory of Disaster Medicine Technology, Tianjin, China

Contributions: (I) Conception and design: Q Lu, Y Zhao, H Fan, S Hou; (II) Administrative support: Y Zhao, H Fan, S Hou; (III) Provision of study materials or patients: Q Lu, Y Zhao, H Fan; (IV) Collection and assembly of data: S Huang, S Yu, M Shi; (V) Data analysis and interpretation: S Huang, J Li, Y Liang; (VI) Manuscript writing: All authors; (VII) Final approval of manuscript: All authors.

[#]These authors contributed equally to this work.

Correspondence to: Yanmei Zhao, MD; Haojun Fan, MD; Shike Hou, MD. School of Disaster and Emergency Medicine, Tianjin University, No. 92 Weijin Road, Nankai District, Tianjin 300072, China; Tianjin Key Laboratory of Disaster Medicine Technology, Tianjin, China. Email: zhaoyanmei@tju.edu.cn; fanhj@tju.edu.cn; houshike@tju.edu.cn.

Background: Sulforaphane (SFN) has been demonstrated to exert a protective role in various diseases. However, the role of SFN in phosgene-induced acute lung injury (P-ALI) remains unclear. This study aimed to explore the role and mechanism of SFN in P-ALI and provide a theoretical basis for the clinical prevention and treatment of P-ALI.

Methods: A mouse model of P-ALI was established followed by phosgene gas inhalation at a dose of 4.17 g/m^3 for 5 min. The survival rate, lung coefficient and hematoxylin and eosin (H&E) staining, lung pathology scoring, and bronchoalveolar lavage fluid (BALF) analysis were performed to evaluate lung tissue damage. The real-time quantitative polymerase chain reaction (RT-qPCR) and Western blotting analysis were utilized to evaluate the relative expression levels of inflammation factors and protein expression.

Results: Compared with the control group, destruction of alveolar structure, pulmonary edema, lung tissue inflammation and oxidative stress occurred after phosgene exposure. After the administration of SFN, the massive exudation of red blood cells and significant thickening of alveolar interstitium were ameliorated, the lung tissue inflammation was improved, and oxidative stress level was reduced. Mechanically, SFN could increase the expression of nuclear factor erythroid 2 (NFE2)-related factor 2 (Nrf2) protein and the downstream heme oxgenase-1 (HO-1) and NAD(P)H:quinone oxidoreductase 1 (NQO1), thereby improving P-ALI. And the Nrf2 inhibitor ML385 attenuated the lung protective effect of SFN.

Conclusions: Phosgene inhalation led to edema, inflammation, and oxidative stress of lung tissue in mice. SFN might ameliorate phosgene-induced lung injury through Nrf2-HO-1/NQO1 signaling pathway.

Keywords: Sulforaphane (SFN); phosgene-induced acute lung injury (P-ALI); inflammation; oxidative stress; Nrf2-HO-1/NQO1 signaling pathway

Submitted May 17, 2024. Accepted for publication Aug 30, 2024. Published online Oct 30, 2024.
doi: 10.21037/jtd-24-819
View this article at: https://dx.doi.org/10.21037/jtd-24-819

Introduction

Phosgene, a chemical warfare agent utilized during World War I, is currently extensively employed in industrial production, such as in the production of insecticides, plastics, pharmaceuticals, pesticides, and isocyanate-based polymers (1). Despite strict regulations on the storage and usage of phosgene, accidental exposure to phosgene still occurs. For instance, a highly toxic phosgene exposure

accident occurred in a DuPont Factory in Belle, West Virginia in 2010, which fatally injured one worker (2). In 2017, a company in Shanghai experienced a phosgene leak accident, which caused 236 patients with phosgene inhalation (3). With approximately 12 million metric tons of phosgene produced globally each year, accidental leakage of phosgene poses a serious threat to the safety of workers and surrounding people.

Phosgene exposure mainly causes damage to the respiratory system. Excessive phosgene inhalation can lead to acute lung injury (ALI), presenting as coughing, chest tightness, wheezing, pulmonary edema, dyspnea, and hypoxemia; severe cases may progress to acute respiratory distress syndrome (ARDS) (1). Currently, treatment for phosgene-induced acute lung injury (P-ALI) involves supportive therapy with no specific therapeutic drug developed (4). However, once a mass poisoning incident occurs, it will put a heavy burden on medical facilities. Therefore, there is an urgent need to identify effective prevention and treatment strategies.

P-ALI is characterized by massive pulmonary edema, epithelial tight junction disruption, surfactant dysfunction, and oxidative stress (5). The molecular mechanism behind P-ALI has not been fully elucidated, and the main possible mechanisms of injury-ALI are the release of inflammatory factors and oxidative stress. After phosgene exposure, the levels of inflammatory cytokines such as tumor necrosis factor-α (TNF-α), interleukin (IL)-1β (IL-1β), IL-6, IL-18, and IL-33 in bronchoalveolar lavage fluid (BALF) and serum were significantly increased, which indicated an inflammatory response in P-ALI (6,7). The uncontrolled inflammatory reaction eventually leads to a cascade of inflammatory changes in the lungs, resulting in ARDS (1).

Highlight box

Key findings

- Sulforaphane (SFN) attenuated inflammation and oxidative stress induced by phosgene.
- The protective effects of SFN were related to the Nrf2-HO-1/NQO1 pathway.

What is known and what is new?

- Excessive phosgene inhalation can result in acute lung injury (ALI).
- SFN attenuated ALI induced by phosgene.

What is the implication, and what should change now?

- Our study provided a theoretical basis for the clinical prevention and treatment of phosgene-induced ALI.

Additionally, oxidative stress is also one of the important mechanisms of phosgene damage, mainly manifested as significantly increased malondialdehyde (MDA) level and superoxide dismutase (SOD) activation, as well as decreased levels of glutathione (GSH) in the lung. This further lead to damage to lung organs (6,8). Inflammation and oxidative stress are key mechanisms underscoring sublethal phosgene injury. Therefore, improvement inflammation and oxidative stress is essential for the prevention of P-ALI.

The nuclear factor erythroid 2 (NFE2)-related factor 2 (Nrf2), a member of the Cap-n-Collar family of basic leucine zipper proteins, is a key transcription factor that regulates antioxidant stress. Under basal conditions, Nrf2 is inhibited by Kelch-like erythroid cell-derived protein with CNC homo-related protein 1 (Keap1) in the cytoplasm (9). When intracellular reactive oxygen species (ROS) are overproduced, Nrf2 dissociates from Keap1 and translocates to the nucleus, where Nrf2 binds to its downstream antioxidant response elements (AREs) to induce transcription of downstream antioxidant genes, such as heme oxgenase-1 (HO-1), glutaredoxin 1 (Grx1), catalase (CAT), and NAD(P)H:quinone oxidoreductase 1 (NQO1) (10). Sulforaphane (SFN), an isothiocyanate derivative present in cruciferous vegetables, is a potent activator of Nrf2 (11). It has been shown to play a protective role in a variety of diseases due to its antioxidant properties. For example, it has been reported that SFN can restore mitochondrial function, cardiac function and activation/differentiation of skeletal muscle satellite cells. It has been considered an effective strategy to protect against muscle and heart dysfunction due to aging (12). Additionally, SFN treatment has shown improvement in long-term sensorimotor and cognitive deficits in ischemic stroke, suggesting a neuroprotective effect of SFN (13). In a lung ischemia-reperfusion (I/R) injury-model, SFN exerts anti-inflammatory effects through the Nrf2/ARE pathway, thus improving lung injury (14). However, the role of SFN in P-ALI has not been studied. As an improvement of inflammation and oxidative stress is essential for the intervention of P-ALI, we hypothesized that SFN also plays a protective role in P-ALI.

In this study, we aimed to explore the role of SFN in P-ALI. At the same time, since SFN is considered as a Nrf2 activator, which indirectly plays an antioxidant role by activating a variety of endogenous antioxidants (15), we also investigated the activation of the Nrf2 signaling pathway after administration of SFN in P-ALI, in order to provide a theoretical basis for the clinical prevention and treatment of P-ALI. We present this article in accordance

with the ARRIVE reporting checklist (available at https://jtd.amegroups.com/article/view/10.21037/jtd-24-819/rc).

Methods

Animals and treatments

Male C57BL/6J mice (weighting 20±2 g, 6–8 weeks old) were purchased from the Beijing Vital River Laboratory Animal Technology Co., Ltd. (Beijing, China), and were housed in standard environmental conditions at 22±2 ℃ under a 12 h light/dark cycle with free access to food and water. All the animal experiments were conducted in compliance with the guidelines of the Tianjin Medical Experimental Animal Care, and animal protocols were approved by the Institutional Animal Care and Use Committee of Yi Shengyuan Gene Technology (Tianjin) Co., Ltd. (protocol number YSY-DWLL-2021061).

Mouse model of phosgene-induced ALI

Phosgene was produced by dissolving triphosgene (Sinopharm Chemical Reagent Co., Ltd., Shanghai China) in cyclohexane (Damao Chemical Reagent Factory Co., Ltd., Tianjin, China) with N,N-dimethyl formamide (Macklin Co., Ltd., Shanghai, China) and released at a constant rate. The animals were placed into an exposure cabinet and allowed to breathe spontaneously, followed by phosgene gas inhalation at a dose of 4.17 g/m^3 for 5 min. Then the animals were placed into separate cabinets with fresh air. Mice were sacrificed 2, 4, 6, 12 and 24 h after phosgene inhalation to confirm that P-ALI model was successfully established.

Experimental groups

Two sets of experiments were carried out. The first set was to investigate the role of SFN in P-ALI. Thirty-five mice were randomly divided into three groups: the control group (n=7), P-ALI group (n=7) and P-ALI + SFN group (n=21). The P-ALI group of mice were exposed to phosgene to establish the P-ALI model. Mice in P-ALI + SFN group were intraperitoneally injected 5 mg/kg (low dose) (n=7), 10 mg/kg (medium dose) (n=7) or 15 mg/kg (high dose) (n=7) SFN 1 h before phosgene exposure. SNF (10 mg/kg) was chosen for the subsequent detection.

The second part of experiment was designed to prove the mechanism of SFN in P-ALI. Mice were randomly assigned to five groups as follows (n=7): the control, P-ALI, P-ALI + SFN, P-ALI + SFN + ML385 and SFN group. The P-ALI, P-ALI + SFN and P-ALI + SFN + ML385 groups of mice were exposed to phosgene as mentioned above. Mice in P-ALI + SFN group were intraperitoneally injected 10 mg/kg SFN 1 h before phosgene exposure. Mice in P-ALI + SFN + ML385 group were intraperitoneally injected 30 mg/kg ML385 1 h before SFN administration and 2 h before phosgene exposure. Mice in the SFN group was intraperitoneally injected 10 mg/kg SFN without phosgene exposure. Twenty-four hours after exposure to phosgene, all mice were sacrificed, and the lung tissue was collected for subsequent experiments.

Histological analysis

Lung tissue was fixed with formalin for 24 h and embedded in paraffin. Then the lung tissue was cut into 4-μm sections and stained with H&E. The stained lung tissue sections were examined under an optical microscope. The severity of lung injury in H&E staining of mouse lung sections based on alveolar congestion, erythrocyte exudation, inflammatory cell infiltration, and pulmonary interstitial thickening were each scored on a scale of 0–4: 0, no injury; 1, mild injury; 2, moderate injury; 3, severe injury; 4, extremely severe injury. Each experiment was performed on a minimum of three animals.

BALF analysis

A 0.5-mL sterile saline was injected into the lungs of mice for repeated suction for 4 times and lavage for 2 times. The collected BALF was immediately centrifuged at 4 ℃ at 12,000 rpm/min for 10 min, the supernatant was collected, and the protein concentration was measured. The cell precipitates were resuspended with 0.1–0.2 mL phosphate buffered saline (PBS) solution. Total cell count was performed with 10 μL suspension. A 5–10-μL suspension was placed on a slide, fixed with methanol, and stained with Giemsa. The neutrophils were counted under an optical microscope.

Total RNA isolation and real-time quantitative polymerase chain reaction (RT-qPCR) analyses

The total RNA of lung tissue was extracted by TRIzol reagent following the manufacturer's protocol. And the RNA was quantified by NanoDrop One ultramicroscopic spectrophotometer (ThermoFisher Scientific, MA, USA).

Table 1 Primers used for RT-qPCR

Target gene	Primer sequence (5'→3')	Length/bp
β-actin	F: AGTGTGACGTTGACATCCGT	20
	R: GCAGCTCAGTAACAGTCCGC	20
IL-1β	F: TGCCACCTTTTGACAGTGATG	21
	R: AAGGTCCACGGGAAAGACAC	20
IL-6	F: TAGTCCTTCCTACCCCAATTTCC	23
	R: TTGGTCCTTAGCCACTCCTTC	21
HO-1	F: GGGCTGTGAACTCTGTCCAA	20
	R: GGTGAGGGAACTGTGTCAGG	20
NQO1	F: GTTTCTGTGGCTTCCAGGTC	20
	R: CGTTTCTTCCATCCTTCCAG	20
SOD1	F: TTCTCGTCTTGCTCTCTCTGG	21
	R: GTTCACCGCTTGCCTTCT	18

RT-qPCR, real-time quantitative polymerase chain reaction; F, forward; R, reverse.

To determine the mRNA expression of target genes, the RNA was reversely transcribed into cDNA using PrimeScript™ RT reagent Kit. Then, LightCycler 96 quantitative PCR instrument (Roche, Basel, Switzerland) and specific primer sequences (*Table 1*) were used for RT-qPCR analysis. The relative expression level of target genes was normalized to that of β-actin, and calculated by the $2^{-\Delta\Delta Ct}$ method.

Western blotting

The lung tissue was lysed in RIPA lysis buffer on ice for 30 min. After centrifugation at 12,000 rpm for 30 min at 4 ℃, the supernatant was collected. Protein concentrations were determined using the bicinchoninic acid (BCA) protein assay kit. After diluted with loading buffer and boiled at 100 ℃ for 10 min, the protein samples were separated by 10% sodium dodecyl sulfate-polyacrylamide gel electrophoresis (SDS-PAGE) and transferred to polyvinylidene fluoride (PVDF) membranes (0.45 μm). The membrane was sealed with 5% nonfat milk at room temperature for 2 h and incubated overnight at 4 ℃ with primary antibody to β-actin (1:10,000), IL-6 (1:1,000), IL-1β (1:800), NQO1 (1:1,000), HO-1 (1:2,000), Nrf2 (1:1,500) and p-Nrf2 (1:2,000). Subsequently, the membrane was washed with tris-buffered saline with Tween 20 (TBST) for three times. Then the second antibody was added (1:300) and incubated at room temperature for 2 h. After washing, protein bands were visualized by chemiluminescence detection enhanced chemiluminescence (ECL) kit. Image-J software was used to analyze the optical density of related protein bands, and β-actin protein bands were used as the standard control.

Measure of ROS levels

ROS levels were measured using dichloro-dihydro-fluorescein diacetate (DCFH-DA). The lung tissue was fully grinding in PBS buffer, and the cell precipitates were collected after centrifugation. Then the cell precipitates were suspended by DCFH-DA and incubated at 37 ℃ for 60 min. After centrifugation at 2,000 g for 10 min, the cell precipitates were collected. Then the cell precipitates were washed with PBS for twice. An excitation/emission wavelength of 500±15/530±20 nm was used to read the fluorescence.

Statistical analysis

SPSS 25.0 (IBM Corp., Armonk, NY, USA) was used for statistical analysis. The data were normally distributed, as determined through Kolmogorov-Smirnov tests, and expressed as the mean ± standard deviation (mean ± SD). Two-group comparisons were performed using Student's *t*-tests, and multiple groups were compared by one way analysis of variance (one way ANOVA), followed by Tukey's multiple comparison tests. The Kaplan-Meier method was used for survival analysis. A statistically significant difference was considered at $P<0.05$.

Results

Successful establishment of phosgene-induced ALI in vivo

To validate that P-ALI model was successfully established, survival rate, lung coefficient, histopathological analysis, lung tissue inflammation and oxidative stress indicators were assessed. As shown in *Figure 1A*, phosgene inhalation resulted in a reduction in the survival rate of mice, with only 58.33% surviving at 24 h post-exposure. The lung coefficient is an important index to measure the degree of pulmonary edema, exhibited a significant increase at 4 h after phosgene exposure and continued to increase over time compared to the control group (*Figure 1B*). Histopathological analysis revealed that 4 h after phosgene

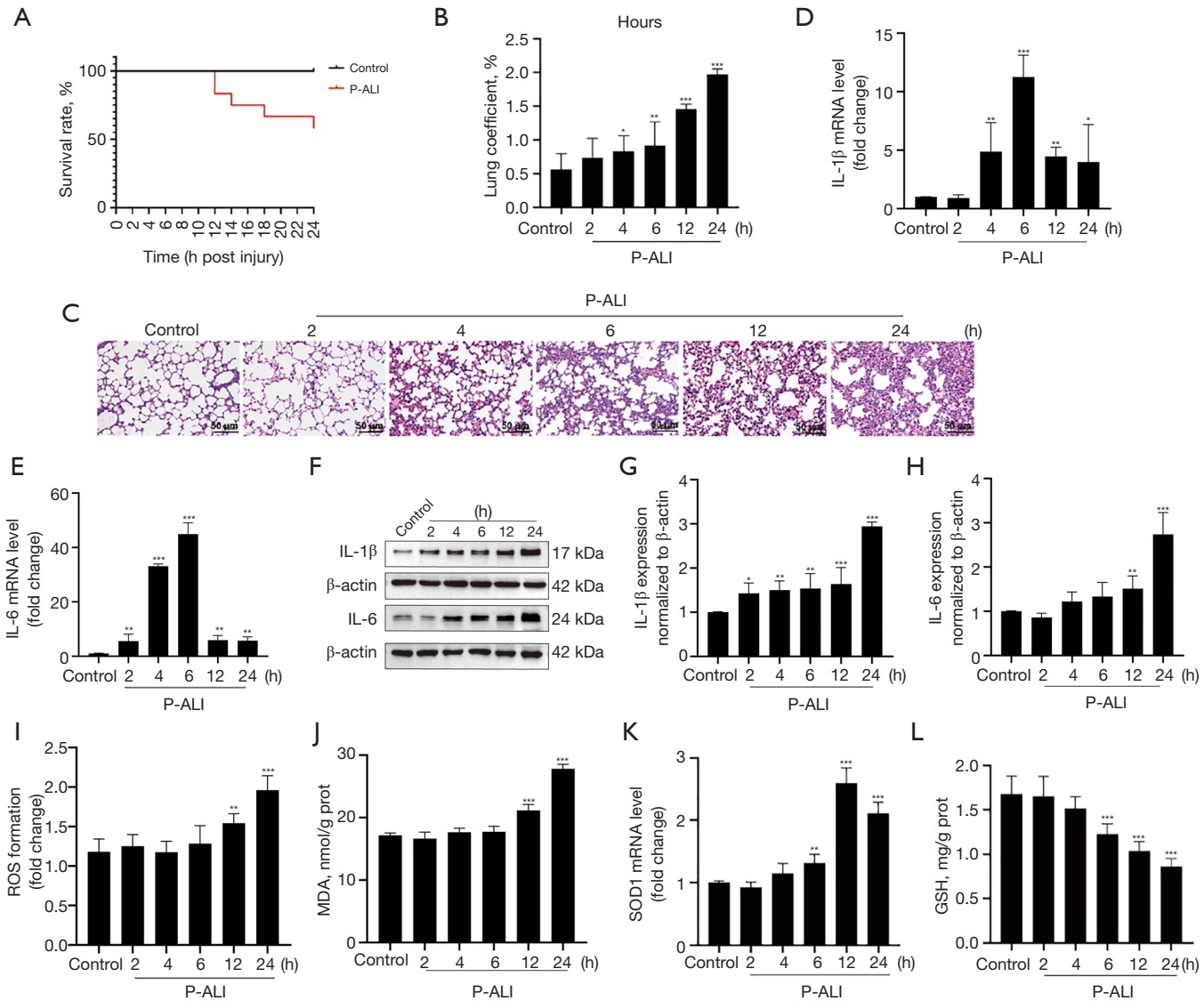

Figure 1 Establishment of P-ALI *in vivo*. (A) Survival rate analysis (n=12). (B) Lung coefficient. (C) H&E staining of lung tissues (n=7). (D-E) Expression levels of IL-1β (D) and IL-6 (E) in lung tissue as determined by RT-qPCR. (F-H) Protein levels of IL-1β and IL-6 in lung tissue, as determined by Western blot assay. (I-L) ROS content (I), MDA concentration (J), SOD1 (K) and GSH (L) activity in the lung tissue. Data were presented as mean ± SD. *, P<0.05; **, P<0.01; ***, P<0.001, compared with the control group. P-ALI, phosgene-induced acute lung injury; IL, interleukin; ROS, reactive oxygen species; MDA, malondialdehyde; SOD, superoxide dismutase; GSH, glutathione; H&E, hematoxylin and eosin; RT-qPCR, real-time quantitative polymerase chain reaction; SD, standard deviation.

inhalation, pulmonary interstitial edema, alveolar septum thickened significantly, a large number of red blood cell leakage and inflammatory cell infiltration occurred, and the severity of lung injury increased with time (*Figure 1C*). The inflammatory factors' results demonstrated a significant elevation in the mRNA and protein levels of IL-6 and IL-1β in mouse lung tissue after phosgene exposure compared to the control group. The mRNA level peaked at 6 h while the protein level reached the peak at 24 h after phosgene exposure (*Figure 1D-1H*). As shown in *Figure 1I-1L*, there were substantial alterations in ROS content (*Figure 1I*), MDA concentration (*Figure 1J*), SOD1 (*Figure 1K*), and GSH (*Figure 1L*) activities within mouse lung tissue after phosgene exposure, indicating that the

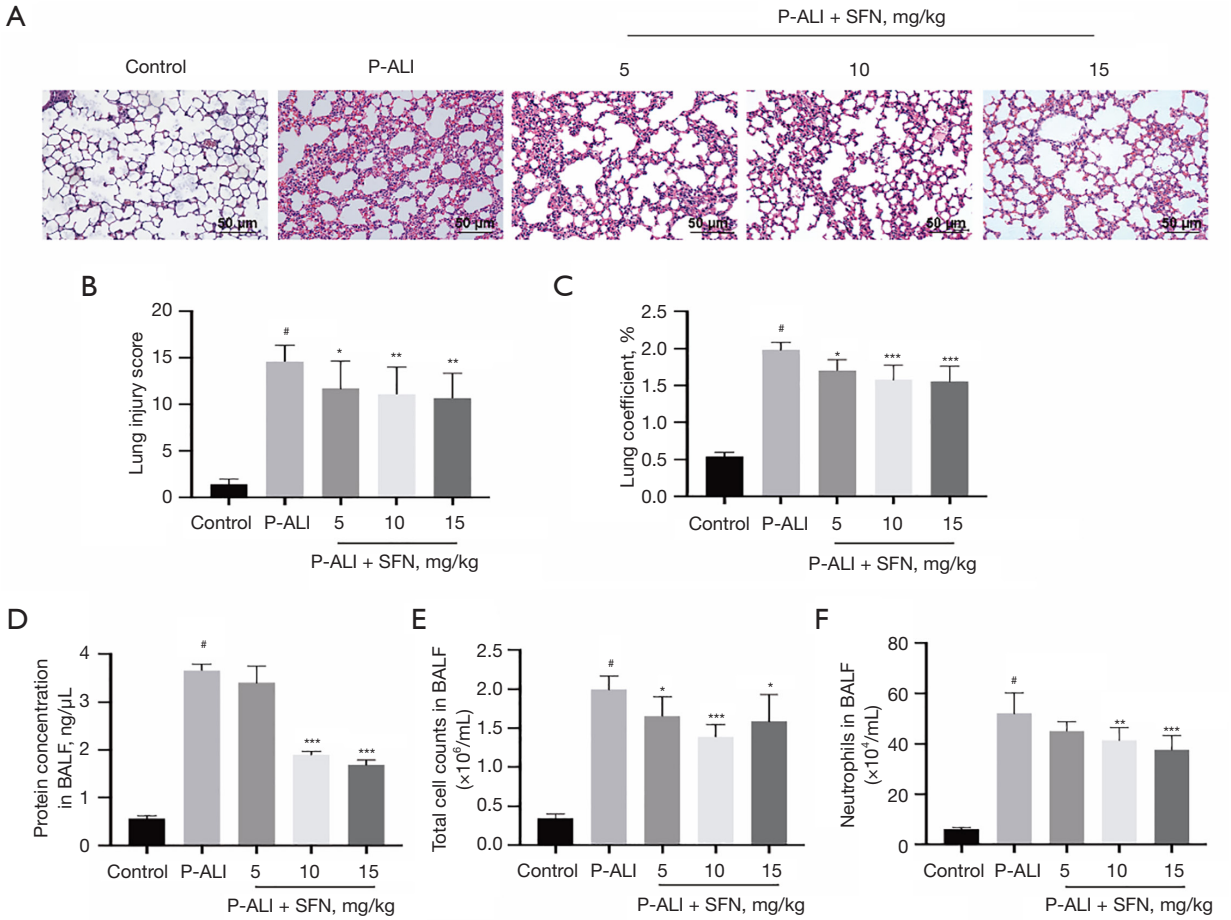

Figure 2 SFN attenuated the severity of P-ALI. (A) H&E staining of lung tissues. (B) Lung injury score. (C) Lung coefficient. (D) The protein level in BALF. (E) Total cell counts in BALF. (F) Neutrophils in BALF. Data were presented as mean ± SD (n=7). #, P<0.05, compared with the control group. *, P<0.05; **, P<0.01; ***, P<0.001, compared with the P-ALI group. P-ALI, phosgene-induced acute lung injury; SFN, sulforaphane; BALF, bronchoalveolar lavage fluid; H&E, hematoxylin and eosin; SD, standard deviation.

REDOX balance in lung tissue of mice may be shifted after phosgene exposure.

SFN attenuated the severity of P-ALI

We examined the severity of ALI at 24 h post phosgene exposure. Histopathological analysis revealed significant lung tissue injury in P-ALI mice, characterized by massive exudation of red blood cells and significant thickening of alveolar interstitium (*Figure 2A*). Administration of SFN at doses ranging from 5 to 15 mg/kg dose-dependently attenuated phosgene-induced lung tissue injury (*Figure 2A,2B*) as well as elevation of lung coefficient (*Figure 2C*). In addition, the protein concentration, total cell counts, and neutrophils in the BALF samples were increased in the P-ALI group, compared to the control group (*Figure 2D-2F*). However, after the treated with medium (10 mg/kg) and high (15 mg/kg) doses of SFN significantly decreased BALF levels (*Figure 2D-2F*), indicating a protective effect of SFN.

SFN attenuate lung tissue inflammation induced by phosgene

Inflammation is one of the mechanisms of phosgene poisoning injury, therefore we examined the effect of SFN on lung tissue inflammation after phosgene inhalation. As shown in *Figure 3*, phosgene induced a significant inflammation response in lung tissue manifested as up-regulation of IL-6 and IL-1β mRNA and protein expression. Medium (10 mg/kg) and high (15 mg/kg) doses

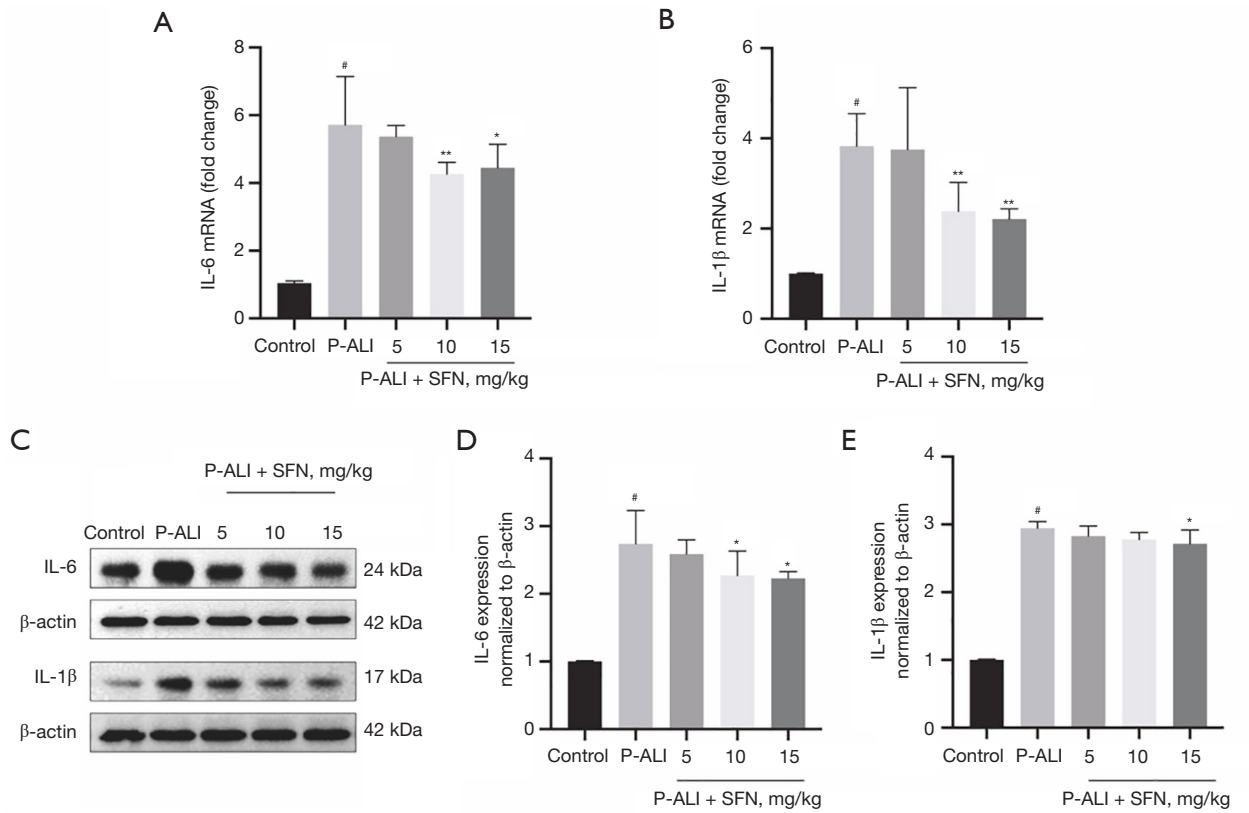

Figure 3 SFN attenuate lung tissue inflammation induced by phosgene. (A,B) Expression levels of IL-6 (A) and IL-1β (B) in lung tissue as determined by RT-qPCR. (C-E) Protein levels of IL-6 and IL-1β in lung tissue, as determined by Western blot assay. Data were presented as mean ± SD (n=7). #, P<0.05, compared with the control group. *, P<0.05; **, P<0.01, compared with the P-ALI group. P-ALI, phosgene-induced acute lung injury; SFN, sulforaphane; IL, interleukin; RT-qPCR, real-time quantitative polymerase chain reaction; SD, standard deviation.

of SFN significantly improved the mRNA expression of proinflammatory cytokine IL-6 and IL-1β induced by phosgene (*Figure 3A*,*3B*). Regarding the protein level, after medium (10 mg/kg) and high (15 mg/kg) doses of SFN administration, the protein level of IL-6 was significantly decreased, however, moderate doses of SFN did not appear to have a significant effect on IL-1β expression after phosgene inhalation (*Figure 3C-3E*).

SFN attenuate oxidative stress induced by phosgene

Oxidative stress is also a major cause of phosgene poisoning injury, thus the effect of SFN on oxidative stress induced by phosgene was also examined. As shown in *Figure 4A*,*4B*, the mice in the model group showed elevated ROS content, which is the main cause of oxidative stress (16), and both medium and high doses of SFN were able to reduce the ROS content after phosgene inhalation. In addition, after exposure to phosgene, the level of MDA, one of the main products of lipid peroxidation and which content is an important index to reflect the degree of lipid peroxidation in tissues, was increased (*Figure 4C*). The activity of the total superoxide dismutase (T-SOD) (*Figure 4D*) and GSH (*Figure 4E*) was significantly decreased in the lungs. Phosgene-induced oxidative stress was attenuated by SFN pretreatment, mainly at medium and high doses.

The protective effects of SFN were associated with the Nrf2-HO-1/NQO1 pathway

To explore the possible mechanisms of SFN in P-ALI, we assessed the Nrf2 signaling pathway, a crucial antioxidant response element (ARE) signaling pathway (17). Compared with the P-ALI group, SFN significantly increased the

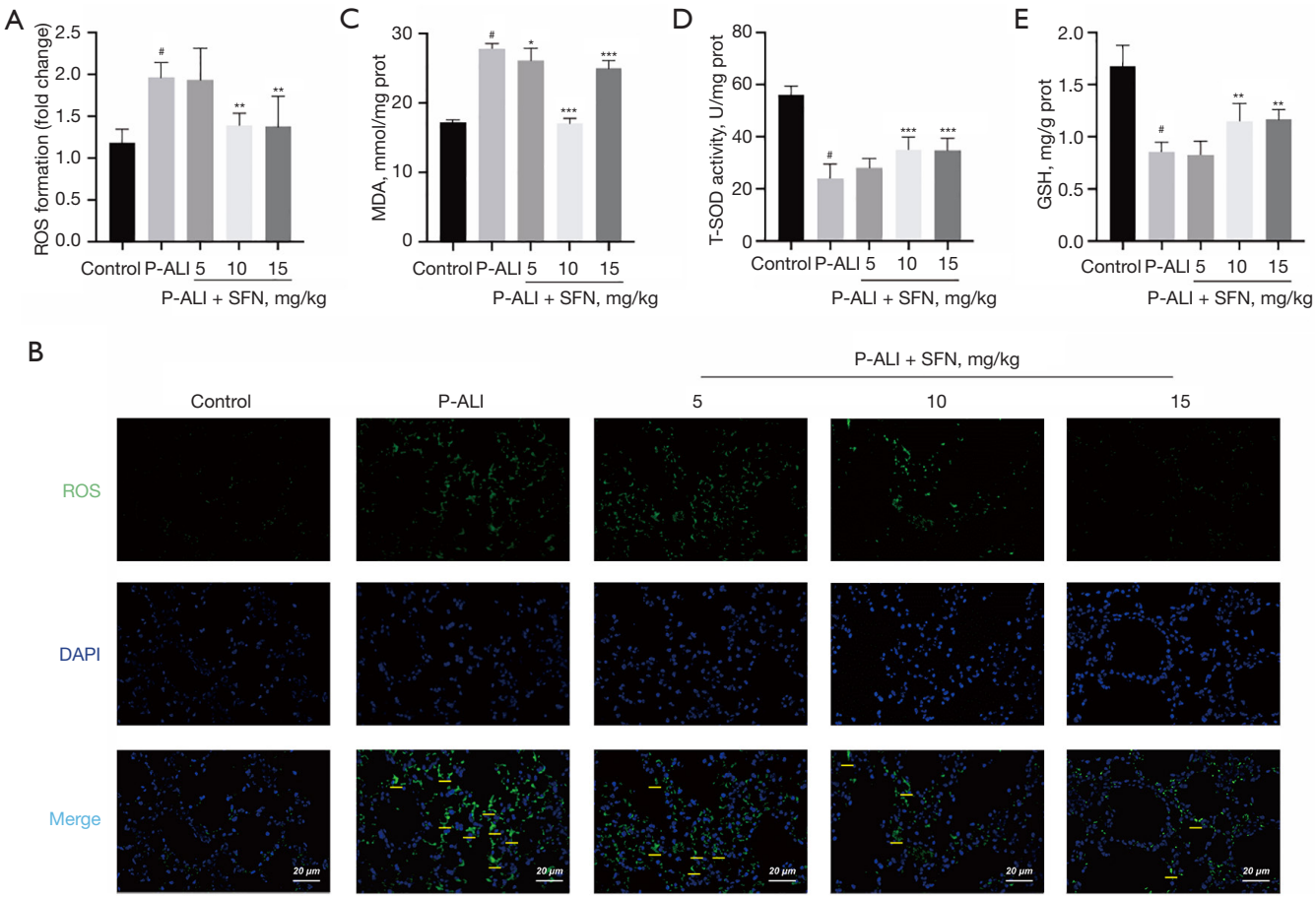

Figure 4 SFN attenuate oxidative stress induced by phosgene. (A,B) DCFH-DA probe determined ROS content in lung tissues of each group, yellow marks indicate ROS positive sites. (C-E) MDA concentration (C), T-SOD (D) and GSH (E) activity in the lung tissue, as determined by chemiluminescence analysis. Data were presented as mean ± SD (n=7). #, P<0.05, compared with the control group. *, P<0.05; **, P<0.01; ***, P<0.001, compared with the P-ALI group. P-ALI, phosgene-induced acute lung injury; SFN, sulforaphane; ROS, reactive oxygen species; DAPI, 4',6-diamidino-2-phenylindole; MDA, malondialdehyde; T-SOD, total superoxide dismutase; GSH, glutathione; DCFH-DA, dichloro-dihydro-fluorescein diacetate; SD, standard deviation.

expression of Nrf2 protein, which can be abolished by Nrf2 inhibitors ML385 (*Figure 5A*,*5B*). Similarly, after SFN administration, the mRNA and protein expression of HO-1 and NQO1, the Nrf2 downstream genes, were increased, however, ML385 could inhibit the effect of SFN (*Figure 5C-5G*).

Nrf2 inhibitor ML385 attenuated pulmonary protective effects of SFN

Subsequently, we explored the role of Nrf2 in lung protection by SFN in phosgene. The survival results showed that SFN increased the survival rate of phosgene poisoning mice from 58.33% to 75%, while ML385 reduced to 66.7% (*Figure 6A*). Furthermore, ML385 significantly attenuate the protective effect of SFN on lung tissue as evidenced by increased pulmonary interstitial edema, thickened alveolar septum, severe destruction of alveolar structure, as well as increased protein concentration along with total cell count and neutrophil count in BALF (*Figure 6B-6E*).

Discussion

Excessive phosgene inhalation can lead to ALI, ARDS, and even death. However, phosgene-induced ALI is usually treated with supportive therapy without any specific

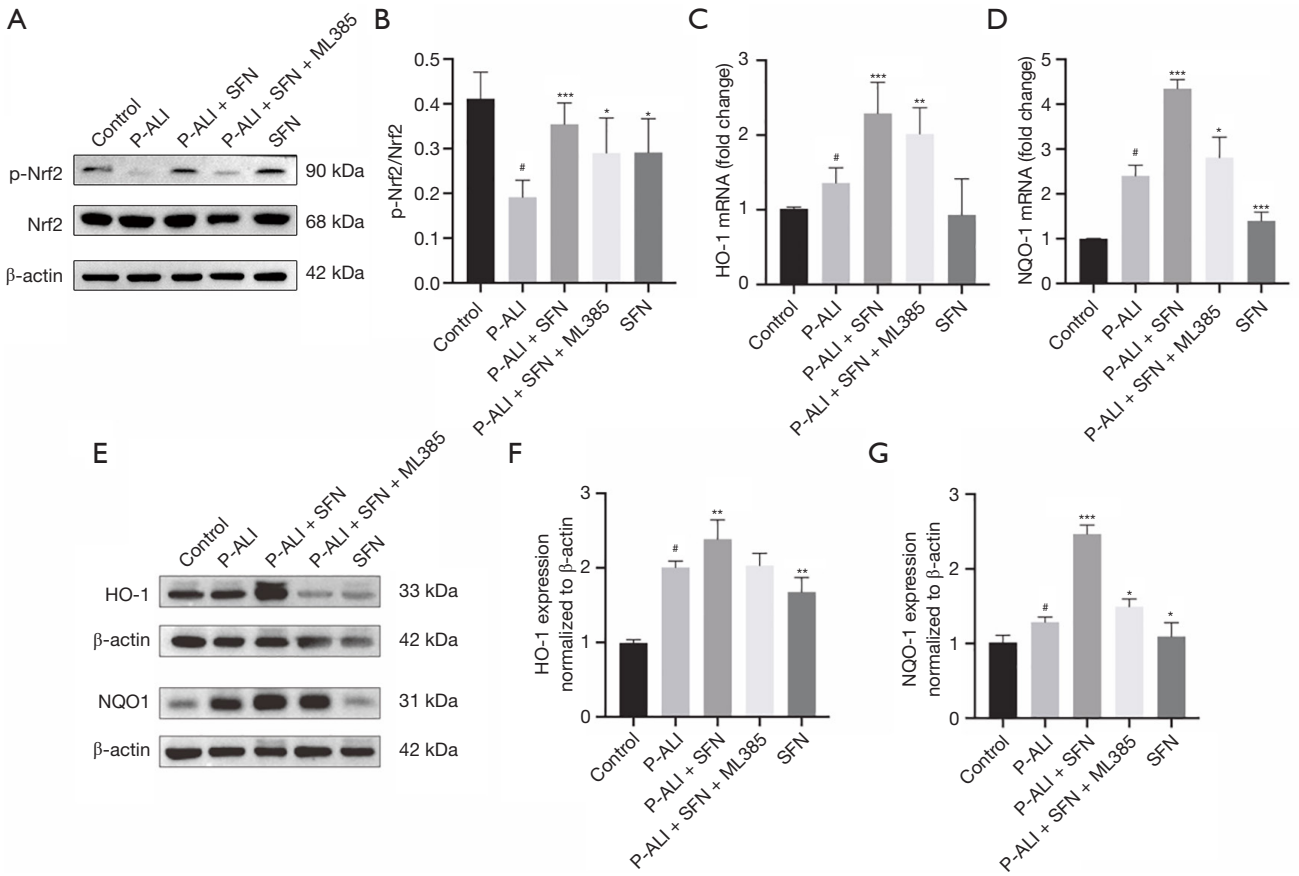

Figure 5 Nrf2-HO-1/NQO1 pathway activation after SFN administration. (A,B) Protein levels of Nrf2 and p-Nrf2 in lung tissue, as determined by Western blot assay. (C,D) Expression levels of HO-1 (C) and NQO1 (D) in lung tissue as determined by RT-qPCR. (E-G) Western blot assay determined the protein expression of HO-1 and NQO1. Data were presented as mean ± SD (n=7). #, P<0.05, compared with the control group. *, P<0.05; **, P<0.01; ***, P<0.001, compared with the P-ALI group. Nrf2, nuclear factor erythroid 2 (NFE2)-related factor 2; P-ALI, phosgene-induced acute lung injury; SFN, sulforaphane; HO-1, heme oxgenase-1; NQO1, NAD(P)H:quinone oxidoreductase 1; RT-qPCR, real-time quantitative polymerase chain reaction; SD, standard deviation.

therapeutic drugs currently available (4). In this study, we successfully established the P-ALI mouse model and explored the effect of SFN on P-ALI. Mechanically, SFN can affect inflammation and oxidative stress through the Nrf2-HO-1/NQO1 pathway to against P-ALI.

Firstly, a mouse model of phosgene inhalation-induced ALI was established. The main manifestations of phosgene poisoning were cough, sputum-like cough, chest tightness, asthma, dyspnea, limb weakness, and consciousness disturbance. Patients with moderate or severe poisoning exhibited significantly accelerated heart rate and respiratory rate, and even developed ARDS (18). In this research, it was found that phosgene inhalation caused pulmonary edema and inflammation, lung ventilation deficiency, pulmonary oxygenation dysfunction, respiratory depression, and even respiratory failure in severe cases. These findings consistent with the clinical results, indicating that we have successfully established a stable mouse model of P-ALI.

Secondly, the study explored the impact of SFN on P-ALI. SFN is a phytocompound belonging to the isothiocyanate family known for its powerful antioxidant, anti-inflammatory, and anti-apoptotic effects, SFN is considered to play an important role in a variety of diseases (19-21). For example, Zhang *et al.* reported that SFN effectively reduced body weight, fasting blood glucose, hyperlipidemia, and improved liver function in mice with insulin resistance induced by a high-fat diet (HFD). They found that SFN significantly reduces oxidative stress mediated by glutathione peroxidase 4 (GPx4) inactivation via activating AMP-activated protein kinase (AMPK) and

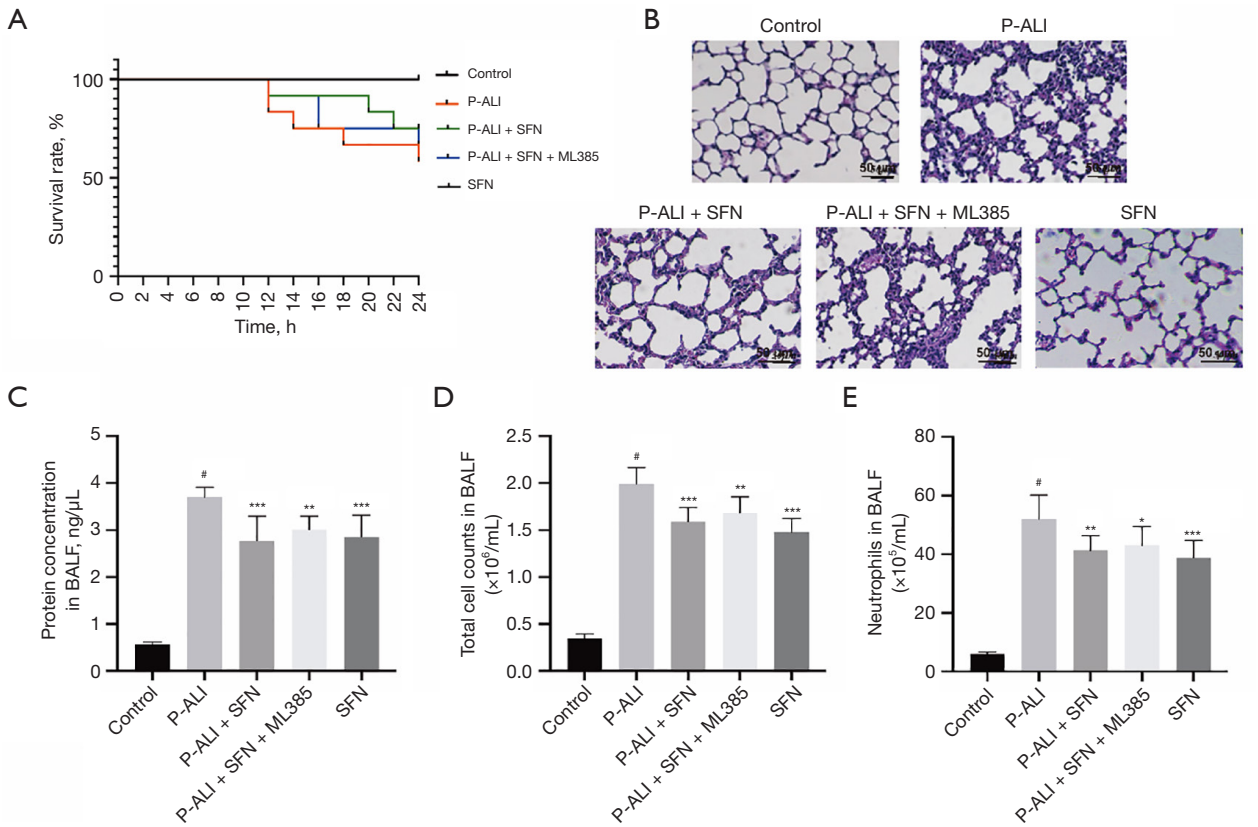

Figure 6 ML385 attenuated pulmonary protective effects of SFN. (A) Survival rate analysis (n=12). (B) H&E staining of lung tissues. (C) The protein level in BALF. (D) Total cell counts in BALF. (E) Neutrophils in BALF. Data were presented as mean ± SD (n=7). #, P<0.05, compared with the control group. *, P<0.05; **, P<0.01; ***, P<0.001, compared with the P-ALI group. P-ALI, phosgene-induced acute lung injury; SFN, sulforaphane; BALF, bronchoalveolar lavage fluid; H&E, hematoxylin and eosin; SD, standard deviation.

Nrf2 signaling pathways (22). In a microglia model, Subedi *et al.* found that SFN exhibited an anti-neuroinflammatory effect on microglia by inhibiting the c-Jun N-terminal kinase (JNK)/activating protein-1 (AP-1)/noncanonical nuclear factor-kappaB (NF-κB) pathway and activating the Nrf2/HO-1 pathway (23). Clinical studies have also shown that SFN can improve conditions such as autism spectrum disorder, pregnancy-induced hypertension in women, muscle soreness and eccentric exercise-related injuries in young people, as well as carcinogen-induced oral cancer (24-27). Therefore, SFN is considered a potential prevention and treatment strategy for numerous diseases. The current research revealed that both medium and high doses of SFN significantly improved phosgene-induced lung tissue inflammation and oxidative stress in mice, which provides a theoretical basis for the clinical use of SFN in P-ALI.

Finally, we found that the protective effects of SFN were associated with the Nrf2-HO-1/NQO1 pathway. Nrf2 is a vital defense element against oxidative stress. When exposed to ROS condition, Nrf2 translocate into the nucleus to up-regulate downstream transcription factors and play the role of anti-oxidative stress. Among the transcription factors downstream of Nrf2, HO-1 and NQO1 are key enzymes responsible for controlling oxidative stress and combatting some toxins (28). SFN, an Nrf2 agonist, can ameliorate lung injury through the Nrf2-HO-1/NQO1 pathway. For example, in a rat sepsis model, SFN supplementation significantly increase the expression of Nrf2 and HO-1 protein, reduce lung oxidative stress during lung sepsis, and alleviate lung injury (29). In this study, we found that SFN significantly increased the mRNA and protein expression of Nrf2, HO-1, and NQO1, compared with the P-ALI group. Furthermore, this increase was abolished by Nrf2 inhibitor ML385. This indicates that the protective effect of SFN on P-ALI is realized through Nrf2-HO-1/NQO1 pathway, and

Nrf2-HO-1/NQO1 pathway could serve as an important target for P-ALI intervention.

Conclusions

In conclusion, we found that SFN attenuates phosgene-induced pulmonary injury, inflammation, and oxidative stress. Additionally, we demonstrated that the protective effect of SFN in alleviating P-ALI is mediated via the Nrf2-HO-1/NQO1 pathway. As there is an urgent need to identify effective prevention and treatment strategies for P-ALI, our study provides a theoretical basis for the clinical use of SFN in P-ALI.

Acknowledgments

We gratefully acknowledge the co-workers of our team. *Funding:* This work was supported by Open Scientific Research Program of Military Logistics (Nos. BLB19J006 and BLB20J009), the National Natural Science Foundation of China (No. 32000877), and Open Project of the Key Laboratory of Trauma and Orthopedics Research Medicine in Henan Province (No. HZKFKT20220504).

Footnote

Reporting Checklist: The authors have completed the ARRIVE reporting checklist. Available at https://jtd.amegroups.com/article/view/10.21037/jtd-24-819/rc

Data Sharing Statement: Available at https://jtd.amegroups.com/article/view/10.21037/jtd-24-819/dss

Peer Review File: Available at https://jtd.amegroups.com/article/view/10.21037/jtd-24-819/prf

Conflicts of Interest: All authors have completed the ICMJE uniform disclosure form (available at https://jtd.amegroups.com/article/view/10.21037/jtd-24-819/coif). The authors have no conflicts of interest to declare.

Ethical Statement: The authors are accountable for all aspects of the work in ensuring that questions related to the accuracy or integrity of any part of the work are appropriately investigated and resolved. All the animal experiments were conducted in compliance with the guidelines of the Tianjin Medical Experimental Animal Care, and animal protocols were approved by the Institutional Animal Care and Use Committee of Yi Shengyuan Gene Technology (Tianjin) Co., Ltd. (protocol number YSY-DWLL-2021061).

References

1. Cao C, Zhang L, Shen J. Phosgene-Induced acute lung injury: Approaches for mechanism-based treatment strategies. Front Immunol 2022;13:917395.
2. DuPont Belle Toxic Chemical Releases. 2010. Available online: https://www.csb.gov/dupont-belle-toxic-chemical-releases-/
3. Zhou XY, Shen J. Application of hospital integrated treatment system in the treatment of public health emergencies-Taking 236 cases of acute chemical poisoning (phosgene) as an example. Chinese Journal of Hygiene Rescue: Electronic Edition 2020;6:301-2.
4. Asgari A, Parak M, Nourian YH, et al. Phosgene Toxicity Clinical Manifestations and Treatment: A Systematic Review. Cell J 2024;26:91-7.
5. Filipczak PT, Senft AP, Seagrave J, et al. NOS-2 Inhibition in Phosgene-Induced Acute Lung Injury. Toxicol Sci 2015;146:89-100.
6. Shao Y, Jiang Z, He D, et al. NEDD4 attenuates phosgene-induced acute lung injury through the inhibition of Notch1 activation. J Cell Mol Med 2022;26:2831-40.
7. He DK, Xu N, Shao YR, et al. NLRP3 gene silencing ameliorates phosgene-induced acute lung injury in rats by inhibiting NLRP3 inflammasome and proinflammatory factors, but not anti-inflammatory factors. J Toxicol Sci 2020;45:625-37.
8. Wang P, Ye XL, Liu R, et al. Mechanism of acute lung injury due to phosgene exposition and its protection by cafeic acid phenethyl ester in the rat. Exp Toxicol Pathol 2013;65:311-8.
9. Chen F, Xiao M, Hu S, et al. Keap1-Nrf2 pathway: a key mechanism in the occurrence and development of cancer. Front Oncol 2024;14:1381467.

10. You L, Peng H, Liu J, et al. Catalpol Protects ARPE-19 Cells against Oxidative Stress via Activation of the Keap1/Nrf2/ARE Pathway. Cells 2021;10:2635.
11. Vanduchova A, Anzenbacher P, Anzenbacherova E. Isothiocyanate from Broccoli, Sulforaphane, and Its Properties. J Med Food 2019;22:121-6.
12. Bose C, Alves I, Singh P, et al. Sulforaphane prevents age-associated cardiac and muscular dysfunction through Nrf2 signaling. Aging Cell 2020;19:e13261.
13. Li Q, Fadoul G, Ikonomovic M, et al. Sulforaphane promotes white matter plasticity and improves long-term neurological outcomes after ischemic stroke via the Nrf2 pathway. Free Radic Biol Med 2022;193:292-303.
14. Zhang L, Wang S, Zhang Y, et al. Sulforaphane alleviates lung ischemia reperfusion injury through activating Nrf 2/HO 1 signaling. Exp Ther Med 2023;25:265.
15. Wei J, Zhao Q, Zhang Y, et al. Sulforaphane-Mediated Nrf2 Activation Prevents Radiation-Induced Skin Injury through Inhibiting the Oxidative-Stress-Activated DNA Damage and NLRP3 Inflammasome. Antioxidants (Basel) 2021;10:1850.
16. Murphy MP, Bayir H, Belousov V, et al. Guidelines for measuring reactive oxygen species and oxidative damage in cells and in vivo. Nat Metab 2022;4:651-62.
17. Culletta G, Buttari B, Arese M, et al. Natural products as non-covalent and covalent modulators of the KEAP1/NRF2 pathway exerting antioxidant effects. Eur J Med Chem 2024;270:116355.
18. Cheng WX, Zhang J, Zhou CY, et al. Analysis of 24 cases of mass acute phosgene poisoning. Chinese Journal of Lung Diseases (Electronic Edition) 2015;8:68-9.
19. Schepici G, Bramanti P, Mazzon E. Efficacy of Sulforaphane in Neurodegenerative Diseases. Int J Mol Sci 2020;21:8637.
20. Russo M, Spagnuolo C, Russo GL, et al. Nrf2 targeting by sulforaphane: A potential therapy for cancer treatment. Crit Rev Food Sci Nutr 2018;58:1391-405.
21. Mangla B, Javed S, Sultan MH, et al. Sulforaphane: A review of its therapeutic potentials, advances in its nanodelivery, recent patents, and clinical trials. Phytother Res 2021;35:5440-58.
22. Zhang Y, Wu Q, Liu J, et al. Sulforaphane alleviates high fat diet-induced insulin resistance via AMPK/Nrf2/GPx4 axis. Biomed Pharmacother 2022;152:113273.
23. Subedi L, Lee JH, Yumnam S, et al. Anti-Inflammatory Effect of Sulforaphane on LPS-Activated Microglia Potentially through JNK/AP-1/NF-κB Inhibition and Nrf2/HO-1 Activation. Cells 2019;8:194.
24. McGuinness G, Kim Y. Sulforaphane treatment for autism spectrum disorder: A systematic review. EXCLI J 2020;19:892-903.
25. Langston-Cox AG, Anderson D, Creek DJ, et al. Sulforaphane Bioavailability and Effects on Blood Pressure in Women with Pregnancy Hypertension. Reprod Sci 2021;28:1489-97.
26. Komine S, Miura I, Miyashita N, et al. Effect of a sulforaphane supplement on muscle soreness and damage induced by eccentric exercise in young adults: A pilot study. Physiol Rep 2021;9:e15130.
27. Bauman JE, Zang Y, Sen M, et al. Prevention of Carcinogen-Induced Oral Cancer by Sulforaphane. Cancer Prev Res (Phila) 2016;9:547-57.
28. Beaver SK, Mesa-Torres N, Pey AL, et al. NQO1: A target for the treatment of cancer and neurological diseases, and a model to understand loss of function disease mechanisms. Biochim Biophys Acta Proteins Proteom 2019;1867:663-76.
29. Zhao B, Gao W, Gao X, et al. Sulforaphane attenuates acute lung injury by inhibiting oxidative stress via Nrf2/HO-1 pathway in a rat sepsis model. Int J Clin Exp Pathol 2017;10:9021-8.

Cite this article as: Lu Q, Huang S, Zhao Y, Yu S, Shi M, Li J, Liang Y, Fan H, Hou S. Sulforaphane attenuates phosgene-induced acute lung injury via the Nrf2-HO-1/NQO1 pathway. J Thorac Dis 2024;16(10):6604-6615. doi: 10.21037/jtd-24-819